

# Dynamical Evolution of Asteroids and Meteoroids Using the Yarkovsky Effect

William F. Bottke, Jr.

*Southwest Research Institute*

David Vokrouhlický

*Charles University, Prague*

David P. Rubincam

*NASA Goddard Space Flight Center*

and

Miroslav Brož

*Charles University, Prague*

Draft of *Asteroids III* chapter

July 30, 2001

## POPULAR SUMMARY

The Yarkovsky effect is a thermal radiation force which causes objects to undergo semimajor axis drift and spin up/down as a function of their spin, orbit, and material properties. This mechanism can be used to (i) deliver asteroids (and meteoroids) with diameter  $D < 20$  km from their parent bodies in the main belt to chaotic resonance zones capable of transporting this material to Earth-crossing orbits, (ii) disperse asteroid families, with drifting bodies jumping or becoming trapped in mean-motion and secular resonances within the main belt, and (iii) modify the rotation rates of asteroids a few km in diameter or smaller enough to explain the excessive number of very fast and very slow rotators among the small asteroids. Accordingly, we suggest that nongravitational forces, which produce small but meaningful effects on asteroid orbits and rotation rates over long timescales, should now be considered as important as collisions and gravitational perturbations to our overall understanding of asteroid evolution.

## 1. The Classical Model of Asteroid Evolution

Over the last several decades, it has been assumed that collisions and gravitational forces are the primary mechanisms governing the evolution of asteroids and meteoroids. Using these processes, it is possible to construct an approximate history of how the main belt and inner solar system asteroid populations have changed over the last several billion years. The main tenets of this model, which we broadly refer to as the "classical" asteroid evolution model, are summarized below.

Asteroids, whose orbits intersect one another in the main belt, occasionally collide with one another at high velocities ( $\sim 5 \text{ km s}^{-1}$ ; *Bottke et al.*, 1994). These events result in cratering and fragmentation, with the collisional physics determining the orbits, spin states, shapes, and internal structures of the surviving bodies. The largest impact events are believed to produce the observed asteroid families (e.g., *Zappalà et al.*, 2002). The orbital positions of family members suggest that some ejecta can be launched at  $\sim$  several  $100 \text{ m s}^{-1}$  (*Zappalà et al.*, 1996). If true, it is plausible that fragments from asteroid collisions, thrown with just the right trajectory and velocity, can be directly injected into powerful or diffusive resonance zones produced by the gravitational perturbations of the planets (*Farinella et al.*, 1993). Numerical studies have shown that test objects in such resonance regions frequently have their eccentricities pumped up to planet-crossing orbits (e.g., *Wisdom*, 1983). Once on planet-crossing orbits, asteroids have their dynamical evolution dominated by resonances and gravitational close encounters with the planets. Some of these asteroids go on to strike the planets, though most impact the Sun or are ejected from the inner solar system via a close encounter with Jupiter (*Gladman et al.*, 1997). If the object is small, it may also be removed via a catastrophic collision. It is believed that most meteorites and near-Earth asteroids are delivered to the inner solar system (and Earth) by this long chain of events.

Up to now, the classical model (CM) has been useful in helping us interpret asteroid data and broadly understand the evolution of asteroid populations. Nevertheless, some predictions its predictions are inconsistent with observations. For example:

**CM Prediction 1:** Since fresh ejecta is directly injected into chaotic resonances, and the dynamical lifetime of bodies placed in powerful resonances are generally a few Myr or less (*Gladman et al.*, 1997), we should expect to see an abundance of meteorites with short cosmic-ray exposure (CRE) ages (i.e., only a few Myr) and a paucity of long-lived meteorites.

**Observation 1:** Relatively few meteorites have CRE ages less than  $\sim 10$  Myr. Most stony meteorites have CRE ages between  $\sim 10$ -100 Myr, while iron meteorites have CRE ages between  $\sim 0.1$ -1.0 Gyr (*Caffee et al.*, 1988; *Marti and Graf*, 1992). In general, CRE ages are comparable to, or longer than, the average dynamical lifetime of Earth-crossing asteroids ( $\sim 10$  Myr; *Gladman et al.*, 1997; *Migliorini et al.*, 1997; *Morbidelli and Gladman*, 1998).

**CM Prediction 2:** There are roughly 5000-6000 km-sized asteroids crossing the orbits of the

terrestrial planets (*Bottke et al.*, 2001a). These bodies have a wide range of taxonomic types (e.g., *Binzel et al.*, 2001). To keep this population in steady state, disruption events among large, spectrally diverse asteroids must be frequent, particularly since these are the only events capable of injecting km-sized fragments into suitable resonant "escape hatches". Since most of these asteroids come from the inner and central main belt (*Bottke et al.*, 2001a), we should expect these regions to contain numerous asteroid families. Moreover, since the planet-crossing asteroids are "fresh ejecta", they should have a relatively steep size-frequency distribution.

**Observation 2:** Few asteroid families can be found in the inner and central main belt, while most potential parent asteroids for the km-sized inner solar system asteroids reside in dynamically stable regions far from resonant "escape hatches". Modeling results including these constraints suggest that the direct injection of asteroid fragments into resonances is too inefficient to keep the inner solar system asteroid population in steady state (*Zappalà and Cellino*, 2001). In addition, the size-frequency distribution of km-sized near-Earth objects (NEOs) is fairly shallow (*Bottke et al.*, 2000a).

**CM Prediction 3:** Studies of asteroid families suggest that many large fragments are ejected from the impact site at high velocities ( $\sim$  several  $100 \text{ m s}^{-1}$ ), with the smallest fragments traveling the furthest from the cluster-center (*Cellino et al.*, 1999).

**Observation 3:** The peak velocities of size-velocity distributions derived from numerical hydrocode results are generally much lower than those inferred from the orbital positions of asteroid family members (*Pisani et al.*, 1999). Though it is possible hydrocodes are inaccurate, their results have been validated using laboratory impact experiments and underground nuclear explosions (e.g., *Benz and Asphaug*, 1999).

**CM Prediction 4:** Asteroid collisions should produce a wide range of asteroid spin rates. To zeroth order, we would expect the spin rates for large and small asteroids to follow a Maxwellian frequency distribution (e.g., *Binzel et al.*, 1989; *Davis et al.*, 1989).

**Observation 4:** The distribution of spin rates among observed small asteroids ( $D < 10 \text{ km}$ ) contains an excess number of fast rotators and very slow rotators when this data is fit to Maxwellian distribution (*Pravec and Harris*, 2000; *Pravec et al.*, 2002).

We believe there is a connection between these mismatches, and that an important physical mechanism is missing from the classical model, namely how nongravitational forces affect the evolution of asteroids. It is already well-known that the dynamical evolution of dust particles can be explained using Poynting-Robertson drag, a radiation effect which causes small objects to spiral inward as they absorb energy and momentum streaming radially outward from the Sun and then reradiate this energy isotropically in their own reference frame (e.g., *Burns et al.*, 1979; *Dermott et al.*, 2002). It is not as well-known, however, that a different nongravitational force

called the Yarkovsky effect can compel objects between 0.1 m-20 km objects to spiral inward or outward at different rates as a function of their spin, orbit, and material properties, or that a variant of this force can also modify the spin rates of asteroids. As we will show in this chapter, this previously-known but mostly-ignored effect, which can be essentially described as a radiation recoil produced by asymmetrically reradiated thermal energy, has the potential to resolve many of the problems described above. Accordingly, we believe the classical model should now be revised to include nongravitational forces as a third important mechanism, in addition to gravity and collisions, affecting asteroid evolution.

## 2. Introduction to the Yarkovsky Effect

Ivan Osipovich Yarkovsky (1844-1902), a civil engineer who worked on scientific problems in his spare time, first proposed the effect which now bears his name (*Neiman et al.*, 1965). Writing in a pamphlet around the year 1900, Yarkovsky noted that the diurnal heating of a rotating object in space would cause it to experience a force which, while tiny, could lead to large secular effects in the orbits of small bodies, especially meteoroids and small asteroids (*Öpik*, 1951). Yarkovsky's effect is a radiation force, and is the photonic equivalent of *Whipple's* (1950) rocket effect.

Yarkovsky's remarkable insight would have been consigned to oblivion had it not been for the brilliant Estonian astronomer Ernst J. *Öpik* (1893-1985), who read Yarkovsky's pamphlet sometime around 1909. Decades later *Öpik*, recalling the pamphlet from memory, discussed the possible importance of the Yarkovsky effect for moving meteoroids about the solar system (*Öpik*, 1951). (Curiously, *Öpik's* (1976) book, which continues the theme of his 1951 paper, seems to make no mention of Yarkovsky). Following *Öpik* and before its current flowering, research on the Yarkovsky-type effects was pursued in Russia by *Radzievskii* (1952; 1954) and *Katasev and Kulikova* (1980), in the United States by *Paddack* (1969; 1973), *Paddack and Rhee* (1975), *Peterson* (1976), *O'Keefe* (1976), *Slabinski* (1977), *Dohnanyi* (1978), and *Burns et al.* (1979), and in Australia by *Olsson-Steel* (1986; 1987). Additional history can be found in *Hartmann et al.* (1999).

### 2.1. Description of Diurnal Component

The basic idea behind Yarkovsky's diurnal effect is shown in Fig. 1a, which shows a spherical meteoroid in a circular orbit about the Sun. For simplicity, the meteoroid's spin axis is taken to be normal to the orbital plane, so that the Sun always stands on its equator. Insolation heats up the sunward side, with the heat ultimately reradiated into space by the meteoroid (typically in the infrared part of the spectrum, unless the meteoroid is very close to the Sun). An infrared photon carries away momentum when it leaves the meteoroid according to the relation  $p = E/c$ , where  $p$  is the photon's momentum,  $E$  its energy, and  $c$  is the speed of light. Because more energy

and therefore more momentum departs from the hotter part of the meteoroid than the colder, the meteoroid feels a net kick in the direction away from the hotter part.

EDITOR: PLACE FIGURE 1 HERE.

If the meteoroid had no thermal inertia, then the temperature distribution would be symmetrical about the subsolar point and the meteoroid would experience a net force radially outward from the Sun. The only consequence of this force would be to weaken the Sun's grip on the meteoroid. However, all bodies have thermal inertia, which causes a delay, so that the hottest part of the meteoroid is its afternoon side rather than the subsolar point. This is similar to the Earth, where afternoon is the warmest time of day, instead of noon. As a result, the force on the meteoroid has not only a component which is radially outward from the Sun, but also has an along-track component.

This along-track component causes a secular increase in the semimajor axis (and, to a lesser degree, eccentricity) for the prograde sense of rotation shown in the figure, so that over time the tiny Yarkovsky force can profoundly change the orbit. The sign of the diurnal Yarkovsky effect depends on the sense of rotation. If the meteoroid shown in Fig. 1a rotated in the retrograde sense, the orbit would shrink instead of expand. The magnitude of the diurnal effect also depends on how close a body is to the Sun, the tilt of the body's spin axis with respect to the orbital plane, and the body's physical characteristics (i.e., the size of the body, its shape and thermal properties, and how fast it is rotating). The interplay of these factors means that there is an optimal size for maximizing the diurnal Yarkovsky effect for a given rotation speed and thermal structure. A very large object would have a poor area-to-mass ratio; the effect is negligible on a large body like the Earth, for example. On the other hand, the smaller the body, the better the area-to-mass ratio, but at some point the radius becomes so small that the thermal wave penetrates all the way across the body, lessening the temperature differences between the night and day sides and weakening the effect; a slowly rotating dust particle would be an example. For rotation speeds believed to be typical in the solar system, optimal sizes for the Yarkovsky effect range from centimeters to meters.

## 2.2. Description of Seasonal Component

Nearly a century after Yarkovsky wrote his pamphlet a second Yarkovsky effect emerged. While searching for the cause of the secular decay of the orbit of the LAGEOS satellite, it was realized that there had to be a seasonal effect (*Rubincam*, 1987, 1988, 1990) in addition to Yarkovsky's original diurnal effect. The seasonal effect applies not just to Earth satellites like LAGEOS, but also to objects orbiting the Sun.

The seasonal Yarkovsky effect is illustrated in Fig. 1b. As in Fig. 1a, a spherical meteoroid is

assumed to be in a circular orbit about the Sun; but in this case the spin axis lies in the orbital plane. It is the component of force lying along the spin axis which gives rise to the seasonal effect. When the meteoroid is at A (bottom of the figure) the Sun shines most strongly on its northern hemisphere. As with the diurnal effect, there is a delay due to thermal inertia, so that the northern hemisphere is hottest at B. Likewise, the Sun shines most strongly on the southern hemisphere at C but this hemisphere becomes hottest at D. When the along-track force is averaged around the orbit, it turns out to be nonzero. For a body without thermal inertia the along-track force averages to zero when integrated over one revolution about the Sun.

For small orbital eccentricities, the average along-track force always opposes to the motion of the meteoroid. Hence in the small eccentricity regime the seasonal force always acts like drag and causes orbital decay; for this reason the seasonal Yarkovsky effect was originally dubbed "thermal drag" (*Rubincam*, 1987). Unlike the diurnal Yarkovsky effect, the seasonal Yarkovsky effect is independent of the sense of rotation of the meteoroid; reversing its spin does not change the effect's sign. Moreover, the relevant timescale for the seasonal effect is the meteoroid's orbital period, rather than the usually much quicker rotational period involved in the diurnal effect.

The seasonal effect does depend on the body's nearness to the Sun, and on the tilt of the spin axis with respect to the orbit; it vanishes when the spin axis is normal to the orbital plane. Like in the diurnal case, there is an optimum size for maximizing the effect. For instance, for basaltic bodies on circular orbits in the inner main belt, the effect is greatest at about 6 m radius (*Rubincam*, 1998; *Farinella et al.*, 1998a). The seasonal Yarkovsky force also affects the other orbital elements in addition to the semimajor axis. For small eccentricities it tends to circularize the orbit, like atmospheric drag does (*Rubincam*, 1995, 1998; *Farinella and Vokrouhlický*, 1999).

### 3. Theory of the Yarkovsky effect

The Yarkovsky force computation naturally splits into two components: (i) determination of the surface temperature distribution, and (ii) evaluation of the thermal radiation recoil force (or torque if desired). Mathematically-equivalent derivations of this solution can be found in several modern references (*Rubincam*, 1995, 1998; *Vokrouhlický*, 1998a,b, 1999; *Vokrouhlický and Farinella*, 1999; *Bottke et al.*, 2000a). In this chapter, we follow the formalism of *Vokrouhlický* (2001).

Problem (i) above has already been examined within the context of asteroid radiometry, but the Yarkovsky application requires some special care. For example, thermal inertia of the surface material – often omitted in radiometry – must now be included. On the other hand, the complexity of the heat diffusion problem can be reduced (within reasonable errors) by adopting linearization (e.g., small temperature differences are referred to a suitably-chosen mean value). For simple asteroid shapes, this procedure allows us to compute the Yarkovsky force using analytical expressions. Since most applications of the Yarkovsky effect require rapid computations,

it is advantageous to sacrifice some precision for speed. More exact solutions, particularly for irregularly-shaped bodies and/or inhomogeneous thermal parameters, require more sophisticated (and computationally expensive) treatments (*Vokrouhlický and Farinella, 1998, 1999; Spitale and Greenberg, 2001a,b*).

To compute the surface temperature on a body, we use the heat diffusion equations for energy flows inside the body:

$$\nabla \cdot (K \nabla T) = \rho C \frac{\partial T}{\partial t}, \quad (1)$$

or across its surface:

$$(K \nabla T \cdot \mathbf{n}_\perp) + \epsilon \sigma T^4 = \alpha \mathcal{E}, \quad (2)$$

the latter which appears as a boundary condition for the temperature ( $T$ ) determination. Here,  $K$  is the thermal conductivity,  $C$  is the specific heat at constant pressure,  $\rho$  is the material density,  $\epsilon$  is the surface thermal emissivity,  $\sigma$  is the Stefan-Boltzmann constant, and  $\alpha = 1 - A$ , with  $A$  being the Bond albedo. Eq. (2) refers to a surface element with an external normal vector  $\mathbf{n}_\perp$ , while  $\mathcal{E}$  is the flux of solar radiation through this element. Once the insolation function  $\mathcal{E}$  for the surface elements is specified (which requires knowledge of the body's shape and its rotation state) and the material parameters ( $K, C, \rho$ ) are known functions of position or temperature (or are assumed constant), the system of Eqs. (1) and (2) can be solved numerically. The corresponding complexity, and the computer time expenses, however, currently prevent an efficient application of this approach for the orbital perturbation determination.

The principal obstacle for an analytic solution of Eqs. (1) and (2) is the nonlinearity in thermal emission on the surface. It can be removed by assuming that the temperature throughout the body is sufficiently close to a suitably chosen average value  $T_0$ ; (i.e.,  $T = T_0 + \Delta T$  with  $\delta = (\Delta T/T_0) \ll 1$ ). If  $T_0$  is constant, Eqs. (1) and (2) may be rewritten for the  $\delta$  variable, while the fourth-order term in the boundary condition (Eq. 2) may be simplified as  $T^4 \approx T_0^4 (1 + 4\delta + \dots)$ . At this point, we find it useful to scale size and time so that minimum parameters are retained in the mathematical formulation of the problem. For example, dimensional analysis shows that, for a given Fourier term with frequency  $\nu$  in the decomposition of the insolation function  $\mathcal{E}$ , the problem involves two fundamental parameters: (i) the penetration depth of the thermal wave  $\ell_\nu = \sqrt{K/\rho C \nu}$ , and (ii) the thermal parameter  $\Theta_\nu = \sqrt{K \rho C \nu} / (\epsilon \sigma T_\star^3)$  (here  $T_\star$  is the subsolar temperature defined by  $\epsilon \sigma T_\star^4 = \alpha \mathcal{E}_\star$  with  $\mathcal{E}_\star$  being the solar radiation flux at the distance of the body). The thermal parameter  $\Theta_\nu$  is a measure of the relaxation between the absorption and reemission at this frequency (the smaller is the value of  $\Theta_\nu$  the smaller is the difference between these two processes). Assuming a spherical body rotating about an arbitrary axis, the spectrum of the insolation function consists primarily of the "diurnal line" with rotation frequency  $\omega$  (and its multiples) and the "seasonal line" with the mean motion frequency  $n$ . Orbital eccentricity adds

higher multiples of the mean motion frequency, which increases algebraic complexity, but it also weakens the assumption of the linearized approach (temperature changes cannot be represented as small variations around a constant average value). Fortunately, most applications of the Yarkovsky effect involve main belt bodies on low-eccentricity orbits. Assuming a small eccentricity, the solution of the amplitudes of the Fourier representation of  $\delta$  as a function of the spatial coordinates can be then worked out analytically.

Having solved the temperature  $T$ , or the linearized quantity  $\delta$ , distribution at the surface of the body, we can proceed to compute the recoil force (or torque) due to the thermal radiation (i.e., Yarkovsky force). Assuming isotropic (Lambert) emission, the corresponding force per unit of mass is given by

$$\mathbf{f} = -\frac{2}{3} \frac{\epsilon \sigma}{mc} \int_S dS(u, v) T^4 \mathbf{n}_\perp, \quad (3)$$

where the integration is to be performed over the whole surface parametrized by a system of coordinates  $u$  and  $v$  (such as the longitude and latitude in the spherical case),  $m$  is mass of the body and  $c$  the light velocity. The integral in (3) may be evaluated numerically, or we may again refer to linearization of the fourth-power of the temperature as mentioned above and perform the integration analytically. Adopting a local coordinate system with the  $z$ -axis aligned with the body's spin axis and the  $xy$ -axes in its equatorial plane, the linearized solutions suggest a useful classification of two variants of the Yarkovsky force: (i) the out-of-spin components of the Yarkovsky acceleration ( $f_x, f_y$ ) depend primarily on the rotation frequency  $\omega$  (with typically unimportant splitting  $\omega \pm n$  due to the orbital motion; *Vokrouhlický, 1999*), while (ii) the spin-aligned component of the Yarkovsky acceleration  $f_z$  depends only on the mean motion  $n$ . The former Yarkovsky-acceleration components are thus called “diurnal”, while the later is called “seasonal” (and they correspond to the qualitative concepts discussed in Sec. 2). It should be noted that splitting the Yarkovsky effect into these two variants is an artifact of the linearized solution. In the more complete formulation, the effects are coupled.

Yarkovsky accelerations primarily change a body's semimajor axis  $a$ . Since the perturbation is usually small, we average the variation in  $a$  over one revolution. Assuming a spherical body with radius  $R$ , and neglecting eccentricity  $e$ , the averaged diurnal and seasonal perturbations on  $da/dt$  are:

$$\left(\frac{da}{dt}\right)_{\text{diurnal}} = -\frac{8\alpha}{9} \frac{\Phi}{n} F_\omega(R', \Theta) \cos \gamma + \mathcal{O}(e), \quad (4)$$

$$\left(\frac{da}{dt}\right)_{\text{seasonal}} = \frac{4\alpha}{9} \frac{\Phi}{n} F_n(R', \Theta) \sin^2 \gamma + \mathcal{O}(e), \quad (5)$$

The total  $da/dt$  rate is the superposition of the two variants. The albedo-factor  $\alpha$  in Eq. (4) and Eq. (5) is close to that in Eq. (2) (*Vokrouhlický and Bottke, 2001*),  $\Phi = \pi R^2 \mathcal{E}_0 / (mc)$  is the



usual radiation pressure coefficient, and  $\gamma$  is obliquity of the spin axis. The function  $F_\nu(R', \Theta)$  depends on the radius of the body  $R$ , scaled by the penetration depth  $\ell_\nu$  of the thermal wave ( $R' = R/\ell_\nu$ ), and the thermal parameter  $\Theta_\nu$ , both corresponding to the frequency  $\nu$ . For the diurnal effect,  $\nu = \omega$ , while for the seasonal effect,  $\nu = n$ . Note that apart from the different frequency,  $F$  is the same in Eqs. (4) and (5). The explicit form of  $F$ -function may be found in the literature (e.g. Vokrouhlický, 1998a, 1999). Here, we restrict ourselves to mention its dependence on the thermal parameter:

$$F_\nu(R', \Theta) = -\frac{\kappa_1(R') \Theta_\nu}{1 + 2\kappa_2(R') \Theta_\nu + \kappa_3(R') \Theta_\nu^2}, \quad (6)$$

with  $\kappa_1$ ,  $\kappa_2$ , and  $\kappa_3$  analytic functions of  $R'$ . The frequency-index of  $F$  reminds us that both the scaling factor  $\ell_\nu$  of  $R$  and the thermal parameter  $\Theta_\nu$  depend on a given frequency. This parameter principle difference between the diurnal and seasonal Yarkovsky effects.

The  $da/dt$  rates listed above give us a basic understanding of how the Yarkovsky perturbations depend on a number of parameters:

- *Obliquity dependence:* Since the  $F$ -functions are always negative (i.e., thermal reemission lags behind the absorption) the seasonal Yarkovsky effect always produce a net decrease in  $a$ . The seasonal effect is maximum at  $90^\circ$  obliquity and nil at  $0^\circ$  (or  $180^\circ$ ) obliquity. On the other hand, the diurnal effect may lead to both a net increase in  $a$  (for  $\gamma < 90^\circ$ ) or a net decrease in  $a$  (for  $\gamma > 90^\circ$ ). The effect is maximum at  $0^\circ$  (or  $180^\circ$ ) obliquity and nil for  $90^\circ$  obliquity.
- *Size dependence:* The Yarkovsky effect vanishes for both very small and very large objects. For large objects,  $(da/dt) \approx \Theta/R'$ ; where the  $\approx 1/R$  dependence is a function of body's cross-section over its mass. For small objects,  $(da/dt) \approx R'^2/\Theta$ . The maximum drift in  $a$  occurs when  $R' \approx 1$  (i.e., when the body's size is comparable to the penetration depth of the corresponding thermal wave).
- *Surface-conductivity dependence:* Surface conductivity  $K$  is the major thermal material parameter that influences the strength of the Yarkovsky effect. It ranges from very low values for highly porous or regolith-like surfaces ( $\approx 0.001 \text{ W m}^{-1} \text{ K}^{-1}$ ), to moderate values for bare-rocks such as ordinary chondrites or icy objects ( $\approx 1 \text{ W m}^{-1} \text{ K}^{-1}$ ), up to high values for iron-rich objects like iron meteorites ( $\approx 40 \text{ W m}^{-1} \text{ K}^{-1}$ ). Variations of  $K$  modify  $\ell_\nu$  and  $\Theta_\nu$ . At low conductivities, we expect that  $\Theta$  will be small and  $R'$  large, since the penetration depth of the corresponding thermal wave decays to zero. Thus,  $(da/dt) \approx \Theta$  and the Yarkovsky effect disappears. For high conductivities, the thermal parameter diverges and the scaled radius of the body tends to zero, since the penetration depth of the corresponding thermal wave diverges. Thus,  $(da/dt) \approx R'^2/\Theta$ , yielding very fast decay of the Yarkovsky

effect as the body is driven toward thermal equilibrium. Maximum  $da/dt$  rates occur when both  $R' \approx 1$  and  $\Theta \approx 1$ .

- *Solar-distance dependence:* The Yarkovsky effect decreases with increasing distance to the Sun. In case of the diurnal effect, objects are usually in the high- $\Theta$  and high- $R'$  regime, so that  $(da/dt) \approx \Phi/(n\Theta)$ . From the functional dependence of  $\Phi$ ,  $n$  and  $\Theta$  on  $a$ , we derive  $(da/dt) \approx a^{-2}$  (e.g. *Radzievskii*, 1952; *Peterson*, 1976). Thus, the diurnal effect decays very fast with increasing distance from the Sun, with very slowly rotating bodies a possible exception. A comparable analysis for the seasonal effect is more involved since  $F_n$  cannot be approximated as  $\approx 1/\Theta$ . An example of this would be 0.1-1 km icy bodies in the Kuiper belt, whose seasonal  $da/dt$  drift rates become much shallower as a function of distance from the Sun. This surprising result occurs because the penetration depth of the seasonal thermal wave  $\ell_n$  increases to  $\sim 0.1$  km.

#### 4. Semimajor axis mobility of asteroid fragments

Using the above equations, *Farinella and Vokrouhlický* (1999) computed the average semimajor axis displacement ( $\Delta a$ ) of main belt meteoroids and asteroids caused by the Yarkovsky effect before undergoing a catastrophic disruption (Fig. 2). The collision lifetime of the objects,  $\tau_{disr}$ , was assumed to be  $\tau_{disr} \simeq 16.8 \sqrt{R}$  Myr, with  $R$  being the body's radius in meters. The objects were started with random obliquity orientations ( $\gamma$ ), but were also assumed to go through spin axis reorientation events via non-disruptive impacts. The characteristic timescale of these events was assumed to be  $\tau_{rot} \simeq 15.0 \sqrt{R}$  Myr (*Farinella et al.*, 1998a). Rotation rates were assumed to be correlated with size through the relation  $P = 5 R$  where  $P$  is the rotation period in seconds and  $R$  the radius in meters. Since surface conductivity  $K$  for asteroids are essentially unknown, several different values of  $K$  were selected.

EDITOR: PLACE FIGURE 2 HERE.

We point out several interesting results from Fig. 2. (i) Except from the high-strength iron objects, the maximum expected drift distance was on order of 0.1 AU. (ii)  $\Delta a$  becomes smaller for large bodies (down to 0.01 AU at  $R \simeq 5 - 10$  km), but much less selective as far as the surface conductivity is concerned. (iii) High-conductivity objects (curve 4 in Fig. 2) have maximum mobility for  $R \approx 10$  m, primarily because of the seasonal Yarkovsky effect (*Rubincam*, 1998; *Farinella et al.*, 1998a). (iv) Characteristic  $\Delta a$  values of  $\approx 0.1$  AU for smaller asteroids and  $\approx 0.01$  AU for km-sized asteroids have important dynamical consequences. For instance, 0.1 – 0.2 AU is a typical distance that a main belt meteoroid might have to travel to reach a powerful main belt resonance. Similarly, 0.01–0.02 AU is a typical semimajor axis span of asteroid families, whose observed components are dominated by multi-km bodies. More details about these applications will be given below.

## 5. Applications of the Yarkovsky effect

### 5.1. Delivery of meteoroids from the main belt to Earth

The original motivation behind the Yarkovsky effect was related to the transport of small bodies from the main belt to Earth (*Öpik*, 1951; *Radzievskii* 1952; *Peterson*, 1976). At the time of these papers, it was unclear whether collisional and dynamical processes were efficient enough to explain the overall flux of meteorites reaching Earth, let alone the cosmic-ray exposure (CRE) ages of stony meteorites (e.g., *Wetherill*, 1974). For this reason, these researchers hypothesized that the Yarkovsky effect might deliver meteoroids from the main belt to Earth via a slow decay of their semimajor axes. The timescales involved with this scenario, however, were too long to be considered practical, particularly when reasonable meteoroid rotation rates were used.

The apparent solution to this meteoroid delivery problem was found in the pioneering works of Williams (see *Wetherill*, 1979) and *Wisdom* (1983), who showed that powerful mean-motion and secular resonances in the inner main belt could potentially move main belt bodies onto Earth-crossing orbits within relatively short timescales ( $\sim 1$  Myr). Thus, a plausible scenario for explaining the CRE ages of stony meteorites became the following: (i) collisions in the main belt inject fragments into resonances, (ii) the fragments evolve onto Earth-crossing orbits via resonant motion, (iii) close encounters remove the objects from resonance, and (iv) the objects wander the inner solar system for 10-100 Myr before striking the Earth, being ejected by Jupiter, or experiencing a collisional disruption event. Since Monte-Carlo code results verified the main components of this model (e.g., *Wetherill*, 1985), the Yarkovsky effect came to be viewed as an unneeded complication and was summarily dropped from consideration by most dynamicists.

Problems with this scenario began to present themselves in the 1990's, as fast workstations and efficient numerical integrations codes began to overtake Monte-Carlo codes as the dominant means of tracking the evolution of small bodies in the solar system. The major blows came from *Farinella et al.* (1994), who showed that many resonant objects strike the Sun, and *Gladman et al.* (1997), who showed that bodies escaping the main belt via the 3:1 mean-motion resonance with Jupiter or the  $\nu_6$  secular resonance only had a mean dynamical lifetime of  $\sim 2$  Myr. As described in the Introduction, these lifetimes are largely discordant with the CRE ages of stony and iron meteorites (e.g., *Morbidelli and Gladman*, 1998).

*Farinella et al.* (1998a), however, recognized that the explanation to the CRE problem might be the Yarkovsky effect, since it could slowly deliver material to powerful resonances inside the main belt.<sup>1</sup> As these bodies drifted towards an escape hatch (typically 0.05–0.15 AU), they would be hit by cosmic rays, which would push their CRE ages into the appropriate range. In

---

<sup>1</sup>Note that this scenario had been previously suggested by both *Peterson* (1976) and *Afonso et al.* (1995). Unfortunately, the implications of their work were overlooked, primarily because (i) the CRE ages of stony meteorites were consistent with dynamical lifetimes derived from Monte-Carlo codes (i.e., *Wetherill*, 1985) and (ii) results from more accurate numerical integration codes were not yet in hand (e.g., *Dones et al.*, 1999).

addition, because iron meteorites have very different thermal conductivities than stones, their  $da/dt$  rates are slow enough to explain their long CRE ages (0.1-1.0 Gyr). Thus, the Yarkovsky effect provides a natural explanation for the paucity of short CRE ages among stony meteorites and the differences in the observed CRE ages of stony and iron meteorites.

The dynamical evolution of main belt meteoroids can be surprisingly complex. As described in the previous section, the drift rate for meter-size stones in the main belt is  $\pm(0.01-0.001)$  AU Myr<sup>-1</sup>, depending on their spin axis orientation, spin rate, and thermal properties. Numerical integration work by *Bottke et al.* (2000a) and *Brož et al.* (2001) have shown that these  $da/dt$  drift rates are fast enough to allow meteoroids to "jump-over" most weak resonances, effectively accelerating their drift rate. Most meteoroids will spiral inward or outward until they become trapped in a powerful resonance too chaotic to jump (e.g., the 3:1 or  $\nu_6$  resonance). En route, some may become temporarily trapped in weak mean-motion or secular resonances, allowing their  $e$  and  $i$  values to undergo secular changes while  $a$  remains fixed. If a meteoroid's  $e$  oscillations reach a high enough amplitude, it may escape the main belt via a close encounter with Mars. Additional complications come from non-disruptive collisions, since they can modify the meteoroid's spin axis orientation and spin rate. Thus, objects drifting via the Yarkovsky effect may well reverse course and speed several times before reaching a powerful resonance. Fig. 3 shows what a representative journey might look like.

EDITOR: PLACE FIGURE 3 HERE.

Although the dynamical evolution of individual meteoroids via the Yarkovsky effect requires careful work, the evolution of large "swarms" of fragments, released by catastrophic break-up events or impacts on large asteroids in the main belt, can be modeled statistically. To this end, the most successful effort so far to combine dynamics, collisions, and the Yarkovsky effect into a meteoroid evolution code has been the work of *Vokrouhlický and Farinella* (2000). In their model, they started with a size distribution of small bodies ejected from a chosen parent asteroid, with each body having its own spin rate and spin axis orientation. Using simplified dynamics, they tracked these bodies across the inner main belt to the 3:1 or  $\nu_6$  resonance, assuming that their  $da/dt$  drift rates were not influenced by smaller resonances. Collisions were also included, with random impact events producing cascades of new fragments from the disruption of the existing bodies. When the objects reached the 3:1 or  $\nu_6$  resonance, Yarkovsky evolution was shut off and the bodies were delivered to Earth via statistical results taken from the numerical simulations of *Morbidelli and Gladman* (1998).

The combination of the two studied phenomena – Yarkovsky drift and collisional dynamics – was found to efficiently supply the 3:1 and  $\nu_6$  resonances with small asteroid fragments from nearly all locations in the inner and central main belt. Direct injections, considered in "pre-Yarkovsky" studies (e.g., *Farinella et al.*, 1993), only seem important when a source is close a resonance. Moreover, the flux of objects to the resonances is, contrary to the direct-injection scenario,

spread over hundreds of Myr, as the collisional cascade creates fast- drifting fragments from larger, slower-drifting progenitors. For example, *Vokrouhlický and Farinella's* results indicate that 50-80 % of the mass of the initial population of bodies released in the Flora-region are transported to resonances (dominantly the  $\nu_6$  resonance) over 0.5 to 1 Gyr.

Another important result from this model is that the distribution of accumulated CRE ages in the population of fragments reaching Earth is in reasonable agreement with observations (e.g., *Marti and Graf, 1992; Welten et al., 1997*). In general, the CRE age histograms are found to depend on the age of the last event capable of dominating the local Earth swarm. Relatively old events are likely to generate the background CRE age profiles (like in the case of L-chondrites) peaked at 20–50 Myr for stones and 200–500 Myr for irons, while comparatively recent and large events may create discrete peaks in the CRE age distributions (such as the 7–8 Myr prominent peak for the H-chondrites). In the latter case, the bulk of the original fragment population may still reside in the main belt and will supply a significant flux of meteorites in the future. Fig. 4 shows comparison of the simulated and observed CRE ages for different types of meteorites and different parent asteroids.

EDITOR: PLACE FIGURE 4 HERE.

## 5.2. Escape of Kilometer-Sized Asteroids from the Main Belt

Dynamical modeling suggests most Earth- and Mars-crossing asteroids ultimately come from the main belt (e.g., *Bottke et al., 2000b, 2001a*). The cratering records of the terrestrial planets suggest this joint population, containing 5000-6000  $D > 1$  km asteroids of various taxonomic types, has been more-or-less in steady state for the last 3 Gyr (*Grieve and Shoemaker, 1994*). The primary sources of these bodies are the 3:1 mean-motion resonance with Jupiter, the  $\nu_6$  secular resonance, and numerous narrow mean motion resonances produced by Mars or the combined effects of Jupiter and Saturn (*Wisdom, 1983; Morbidelli and Gladman, 1998; Migliorini et al., 1998; Morbidelli and Nesvorný, 1999*). The viability of these sources have been checked using sophisticated numerical integration codes which track test asteroids evolving under the combined perturbations of the Sun and planets for  $\sim 100$  Myr (*Wisdom and Holman, 1991; Levison and Duncan, 1994*).

A possible problem with these simulations, however, is that they do not consider how the test asteroids reach their starting orbits. As described in the Introduction, previous work has assumed that asteroids are thrown directly into resonances by main belt collisions (e.g., *Farinella et al., 1993*). The combined width of resonances in the inner and central main belt, however, is small enough that collisions alone may be unable to keep them filled with debris (*Farinella and Vokrouhlický, 1999*). Dynamical models suggest a shortage of resonant material could eventually lead to a discernible depletion of inner solar system asteroids (*Migliorini et al., 1998; Michel et*

*al.*, 2000). This problem would also be exacerbated by the fact that most potential parent bodies are located far from resonant escape hatches, and that the disruption of large bodies in the inner main belt should produce observable asteroid families.

For these reasons, *Farinella and Vokrouhlický* (1999) postulated that most main belt resonances are restocked with  $D \lesssim 20$  km asteroids via the Yarkovsky effect. This potential solution could explain the spectral diversity of the inner solar system asteroid population (e.g., *Binzel et al.*, 2001) as well as the slope of its size-frequency distribution, which is shallower ( $N(> D) \propto D^{-1.75}$ ; *Bottke et al.*, 2000a) than one might expect if fresh ejecta were being launched directly into resonances ( $N(> D) \propto D^{-3}$ ; *Tanga et al.*, 1999). Explaining observations, therefore, requires that models of asteroid delivery from the main belt to the inner solar system must become increasingly complicated.

To investigate this scenario, *Bottke et al.* (2001b) numerically integrated hundreds of test asteroids in the inner (2.1-2.48 AU) and central (2.52-2.8 AU) main belt with and without the Yarkovsky effect. The orbits of the test asteroids were chosen to be a representative sample of the observed population residing near (but not on) Mars-crossing orbits (perihelion  $q \gtrsim 1.8$  AU). Where possible, these tests duplicated the initial conditions investigated by *Migliorini et al.* (1998) and (*Morbidelli and Nesvorný*, 1999). All of these test asteroids were tracked for at least 100 Myr using a numerical integration code modified to accommodate Yarkovsky thermal forces (*Levison and Duncan*, 1994; *Bottke et al.*, 2000b; *Brož et al.*, 2001). A wide range of asteroid diameters (0.2 km, 0.4 km, 2 km, 4 km, 10 km) were used. Objects in the inner and central main belt were given S-type and C-type albedos, respectively. Thermal conductivities were chosen to be consistent with values expected from regolith-covered asteroids. Random spin axis orientations and size-dependant spin rates were also used (e.g., *Bottke et al.*, 2000a). All these tests were compared to a control case where the Yarkovsky effect was turned off.

*Bottke et al.* (2001b) found that Yarkovsky-driven objects with  $D > 2$  km reached Mars-crossing orbits at the same rate as the control case, despite the fact that the dynamical evolution of individual bodies in each set could be quite different (Fig. 5). For example,  $D = 10$  km objects, with slow drift rates (e.g., Fig. 2), followed dynamical paths which were more-or-less analogous to the results of *Migliorini et al.* (1998) and *Morbidelli and Nesvorný* (1999). In this case, secular increases in  $e$  were caused predominantly by the bodies interacting with overlapping mean-motion resonances near the main belt periphery. On the other hand, resonant trapping does not appear to be the dominant behavior of  $D < 2$  km objects; their faster drift rates allow many of them to jump across many numerous weak resonances as they drift into the Mars-crossing region. In general, small inner main belt asteroids do not stop until they reach the wide and powerful 3:1 mean-motion resonance with Jupiter, the  $\nu_6$  secular resonance, or the Mars-crossing region itself. *Bottke et al.* (2001b) concluded from these results that the Yarkovsky effect was more efficient at driving sub-km bodies out of the main belt than multi-km bodies. The major source regions for sub-km asteroids in the inner solar system should be powerful resonances like the 3:1 or  $\nu_6$  resonances, while an important source for multi-km bodies would be the numerous tiny resonances

scattered throughout the main belt (and possibly secular resonances intersecting asteroid families; see next section). *Bottke et al.* (2001a) estimate that the combined flux of km-sized bodies from these sources is  $\sim 220$  per Myr. This rate is high enough to suggest the Yarkovsky effect, rather than collisional injection, is the dominant mechanism pushing material into resonances. It also suggests that some main belt asteroid sources may produce more large or small objects than other sources. A considerable amount of work will be needed to fully appreciate all the ramifications of this new asteroid delivery scenario.

EDITOR: PLACE FIGURE 5 HERE.

### 5.3. Dispersion of Asteroid Families

Asteroid families are remnants of large-scale catastrophic collisions. They are usually identified by their orbital elements, which tend to be clustered at similar values (e.g., *Bendjoya et al.*, 2002). If one assumes that the semimajor axis distribution of family members has been constant since the formation event, it is possible to deduce the original ejection velocities of the fragments by reconstruction (*Zappalà et al.*, 1996). The inferred velocity distributions from this technique, however, which are on the order of hundreds of meters per second, are inconsistent with ejection velocities derived by other means. For example, laboratory impact experiments, where cm-sized projectiles are shot into targets, and numerical hydrocode experiments, which are capable of simulating hypervelocity collisions among large asteroids, both indicate that typical ejection velocities from asteroid impacts are on the order of several tens of meters (*Benz and Asphaug*, 1999). Whenever high velocities are obtained in hydrocode models, the fragment distribution is dominated by small-and thus unobservable-fragments (e.g., *Pisani et al.*, 1999). These results have been used to suggest that hydrocodes may be unreliable tools for modeling large impact events (*Farinella et al.*, 1998b).<sup>2</sup>

Even if this problem could be set aside, we would still be left with several puzzling aspects of asteroid families. One such enigma is the asymmetric  $(a, e, i)$  distribution of many asteroid families. For example, Fig. 6 shows the distribution of the Koronis family in proper  $(a, e)$ . Note that family members with small proper  $a$  are far less dispersed in proper  $e$  than those with large proper  $a$ , while both ends of the family are truncated by powerful mean-motion resonances with Jupiter (i.e., 5:2 on the left, 7:3 on the right). Dynamical models indicate there are several secular resonances intersecting the right side of the Koronis family, but they are relatively weak. Under the auspices of the classical asteroid evolution model, it is difficult to understand how these

---

<sup>2</sup>Note that recent results by *Michel et al.* (2001) indicate that gravitational re-accumulation of small fragments immediately after a family-forming impact can produce some large fragments, but that their ejection velocities are still too small to explain the orbital distribution of observed families.

resonances could produce the observed distribution, since family members injected into them are unlikely to be displaced very much (0.01-0.02 in  $e$ ), even over Gyr timescales. Thus, the classical model can only explain this distribution (and other comparable features among prominent asteroid families) using anisotropic ejection velocity distributions.

EDITOR: PLACE FIGURE 6 HERE.

A second enigma is the observation that several members of prominent asteroid families are either "on the brink" of entering a resonance (e.g., Koronis family members; *Milani and Farinella, 1995; Knežević et al., 1997*), are already inside a powerful resonances (e.g., Eos family members; *Zappalà et al., 2000*), or are part of the relatively short-lived NEO population (V-type asteroids, which presumably are part of the Vesta family; *Migliorini et al., 1997*). The age of families like Eos, Koronis, and Vesta is thought to be 1 Gyr or more (*Marzari et al., 1995*), making it difficult to understand how these family fugitives reached orbits with such short dynamical lifetimes. Using the classical model, one might assume that secondary fragmentation moved these objects onto their current orbits, but the large size of some of the objects ( $D > 10$  km) makes this scenario improbable.

We believe that the simplest scenario capable of explaining all of these mysteries is Yarkovsky-driven migration of asteroid family members. From the time of their formation, we hypothesize that asteroid families have had their configurations modified by collisions, chaotic diffusion, and, in particular, the Yarkovsky effect. As shown in Fig. 2,  $D \sim 20$  km asteroids may move in semimajor axis on order of  $\pm 0.01$  AU over their collisional lifetimes, while  $D \sim 5$  km asteroids can evolve at twice that rate. Since collisional models suggest that many asteroid families are hundreds of Myrs to Gyrs old (*Marzari et al., 1995, 1999*), the potential drift distances of these objects are in the right ballpark to explain the observed dispersions of most asteroid families. Moreover, since Yarkovsky drift is size-dependent, the family members would eventually take on the appearance that they were launched using a size-dependant velocity distribution. Thus, our new scenario to explain observed asteroid families is a multi-step process. (i) A large asteroid undergoes a catastrophic disruption and ejects fragments at velocities consistent with those found in hydrocode simulations. (ii) The fragments, whose initial orbital dispersion is smaller than currently observed, start drifting under the Yarkovsky effect. The drift rate is a function of each object's size, spin state, and thermal properties. (iii) The fragments jump over or become trapped in diffusive mean-motion and secular resonances, which modify their orbital parameters. Secondary collisions and close encounters between family members and large asteroids like (1) Ceres may also produce some mobility (*Carruba et al., 2000; Nesvorný et al., 2001*). (iv) Family members drifting far enough may fall into powerful mean-motion or secular resonances capable of pushing them onto planet-crossing orbits.

To check our ideas, we have modeled the evolution of several synthetic asteroid families according to constraints described in item (i) above. Because our results are preliminary, we



restrict our discussion solely to our results for the Koronis family. In our simulations, we launched a size distribution of 210 test asteroids ( $1 < D < 20$  km) from (158) Koronis using a Maxwellian velocity distribution. Ejection velocities were  $\lesssim 60$  m/s, far less than the inferred ejection velocities found using the current location of Koronis family members ( $\lesssim 300$  m/s; *Cellino et al.*, 1999). The test asteroids were also given random spin axis orientations, spin periods commensurate with their size, and thermal properties consistent with them being covered by regolith (e.g., *Farinella et al.*, 1998a). These bodies were then numerically integrated for 500 Myr using our Yarkovsky numerical integration code (*Brož et al.*, 2001). Some compromises were made for computational expediency, namely that the test asteroid diameters were chosen so they would migrate a reasonable distance over our integration time.

Fig. 6 shows the results of our simulation. We find that Yarkovsky forces drive many family members through a chaotic sea where resonant jumping/trapping events produce noticeable changes in proper  $e$ , particularly on the right side of the plot. The dramatic jumps near 2.92 AU are caused by interactions with tiny secular resonances (such as  $g - 3g_6 + 2g_5$  or  $g + s - 2g_7$ ). This result seems surprising, since we just claimed above that these secular resonances are too weak to cause significant  $e$  oscillations. In our case, however, the drifting bodies adhere to the shape of the resonance, which happens to be quite steep in  $e$ . Moreover, our bodies traverse this part of the resonance in very little time, explaining why so few family members are found there. Thus, this bizarre but important behavior provides additional support for the idea that asteroid mobility via the Yarkovsky effect must take place.

We believe our simulation approximately reproduces the distribution and span of the Koronis family, while also showing that some Koronis family members could be escaping out of powerful resonances today (i.e., Koronis member (2953) Vysheslavia, a 15 km body, is located so close to the 5:2 resonance that it will be ejected from the main belt within 10 to 20 Myr; *Vokrouhlický et al.*, 2000). The match is not perfect, but this could be caused by a number of factors: (i) we are using bodies which are too small and drift too fast; (ii) we need to extend our integration timescale to several Gyr, the expected age of the Koronis family; (iii) several members of the Koronis family shown in Fig. 6 are actually interlopers; or (iv) our formulation for the Yarkovsky effect is too simplistic. Further work, more sophisticated models, and better observations will be needed to produce a more precise match. Still, that fact that our model reproduces the Koronis family as well as it does, and that models of the Koronis family break-up without Yarkovsky generate very different orbital distributions (e.g., *Michel et al.*, 2001), strongly suggests that the Yarkovsky effect is a primary mechanism distorting the figures of older asteroid families.

#### 5.4. Radiative Spin-Up/Down of Asteroids (YORP Effect)

Besides changing the orbit, Yarkovsky forces can also produce torques which affect the spin rate and spin axis orientation of asteroids and meteoroids. The means by which sunlight alters spin was coined by *Rubincam* (2000) as the *Yarkovsky-O'Keefe-Radzievskii-Paddack* effect, or

YORP for short (*Radzievskii*, 1954; *Paddack*, 1969, 1973; *Paddack and Rhee*, 1975; *O'Keefe*, 1976). YORP comes from two sources: reflection and reemission. *Rubincam* (2000) illustrated how it works using a rotating spherical asteroid with two wedges attached to the equator (Fig. 7). For a Lambertian radiator, the reaction force from photons departing from any given element of area will be normal to the surface. Thus, reradiation of energy from the sphere contributes no torque to the body's rotation, while energy reradiated from the wedges produces a torque because the wedge faces are not coplanar. For the sense of rotation shown in Fig. 7, the wedge-produced YORP torque spins the object up. If the body happened to spin in the opposite sense, the YORP torques would slow it down. Thus, an object must have some "windmill" asymmetry for YORP to work (i.e., it would have no effect on rotating triaxial ellipsoids).

YORP torques can also modify asteroid obliquities, which leads to the concept of the YORP cycle. For the geometry shown in Fig. 7, a fast-spinning asteroid would gradually increase its obliquity as well. When the obliquity becomes large enough, the axial torque changes sign and the object begins to spin down. This can be seen by imagining that the Sun shines down on the object from its north pole, rather than the equator; the wedges must spin it the other way. Hence YORP may spin objects up for a while, but when the obliquity becomes large, they slow down and then perhaps tumble until they reestablish principal axis rotation, with the spin axis presumably pointing in a random direction. Then the cycle begins all over again, such that small solid objects probably avoid the "rotational bursting" envisioned by *Radzievskii*, *Paddack*, and *O'Keefe* (i.e., spinning an solid object so fast that it disrupts). Collisions large enough to modify an asteroid's spin axis orientation may also short-circuit a YORP cycle, potentially putting the object into an entirely different rotation state. Thus, YORP is most likely to be important in regimes where the YORP cycle is faster than the spin axis reorientation timescale via collisions. YORP also naturally drives the rotation away from the principal-axis mode. For km- sized objects, especially if they are gravitational aggregates, the internal dissipation processes could efficiently maintain the principal-axis rotation state, but smaller objects are expected to generally acquire an excitation over the fundamental state (e.g., *Rubincam*, 2000; *Vokrouhlický and Čapek*, 2001).

EDITOR: PLACE FIGURE 7 HERE.

*Rubincam* (2000) found that YORP is strongly dependant on an asteroid's shape, size, distance from the Sun, and orientation. For example, assuming the Sun remains on the equator, asteroid (951) Gaspra, with  $R = 6$  km and  $a = 2.21$  AU, takes 240 Myr go from a rotation period  $P = 12$  h to 6 h (and visa-versa). We call this value the YORP timescale. Now, if we gave (243) Ida the same  $R$  and  $a$  values, it would have a YORP timescale half as big, while a body with Phobos's shape would have a YORP timescale of several Gyr. Clearly, shapes make a big difference, and this parameter can vary over an asteroid's lifetime. The YORP timescale is also size-dependant (i.e., it goes as  $\approx R^2$ ), such that smaller sizes spin up much more quickly. If Gaspra was only  $R = 0.5$  km, its YORP timescale would be a few Myr. Thus, YORP may be very influential for km-sized and smaller asteroids. Finally, YORP is more effective as you move closer

to the Sun. Moving our  $R = 0.5$  km Gaspra to 1 AU allows it to go from  $P = 12$  h to rotational disruption speeds of  $\sim 2$  h (and visa-versa) in  $\sim 1$  Myr. We caution, however, that YORP-induced obliquity torques may double or possibly triple the timescales described above. Moreover, these rates also assume the YORP cycle continues without interruption via collisions, planetary close encounters, etc., and that asteroid thermal properties do not significantly change with size. These real-life complications will be modeled in the future.

If these last YORP timescales are reasonable values for small asteroids, it is plausible that YORP may spin small gravitational aggregates up so fast that they are forced to "morph" into a new shape and/or undergo mass shedding. Since symmetrical shapes increase the YORP timescale, these shape changes may eventually strand some objects close to the rotational break-up limit. If rotational disruption is common, we hypothesize that YORP may supersede tidal disruption and collisions as the primary means by which binary asteroids are produced.

At this point, we can begin to explore the possible connection between asteroid spin rates and the YORP effect. Observations show that  $D > 125$  km asteroid have rotation rates which follow a Maxwellian-frequency distribution, while  $50 < D < 125$  km asteroids show a small excess of fast rotators relative to a Maxwellian and  $D > 50$  km asteroids show a clear excess of very fast and slow rotators (Binzel *et al.*, 1989). More recent observations indicate that  $D < 10$  km asteroids have even more pronounced extrema (Pravec and Harris, 2000; Pravec *et al.*, 2002). These results suggest that one or more mechanisms are depopulating the center of the spin rate distribution in favor of the extremes, and that these mechanisms may be size-dependent.

The possible mechanisms capable of performing these spin modifications are: (i) collisions, (ii) tidal spin-up/down via a close encounter with a planet, and (iii) tidal evolution between binary asteroids, where spin angular momentum is exchanged for orbital angular momentum (with possible escape), and (iv) YORP. The limitations of (i)-(iii) are described in Pravec *et al.*, (2002) and will not be reviewed here. The advantage of YORP over these other mechanisms is that it can naturally produce both slow and fast rotation rates for small asteroids over relatively short timescales, and that it is a size-dependant force, helping to explain why the spin rate distributions change with  $D$ . The disadvantage of YORP is that it does not appear to be capable of significantly modifying the spin rates of large asteroids by itself. A unified model, which includes these processes and YORP, however, might do a reasonable job at explaining the spin rates of large asteroids like (253) Mathilde. The solution is left to future work.

At the time of this writing, we consider YORP studies to be in their infancy. For example, Vokrouhlický and Čapek (2001) recently pointed out that the YORP-evolving rotation state may become temporarily locked in one of the resonances between the precession rate and the proper or forced frequencies of the long-term orbital-plane evolution. These effects may temporarily halt, reverse or accelerate the YORP influence on the obliquity. Future work on the YORP effect must also take into account thermal relaxation, non-principal-axis rotation, and more refined thermophysics (e.g., Spitale and Greenberg, 2001a,b).

## 6. Conclusions and Future Work

The Yarkovsky effect was introduced into planetary dynamics as a possible transportation mechanism for meteorites. Today, we recognize that this effect, working in concert with resonances, may be the primary mechanism by which material is delivered from the main belt to Earth. Moreover, by including the Yarkovsky accelerations into fast numerical integration codes, we are beginning to perceive how asteroid families, the structure of the main belt, and even some asteroid rotation rates (and, as a by-product, asteroid shapes) have been modified by these subtle yet influential forces.

At the present time, the existence of the Yarkovsky effect is mostly based on inferences, such as the statistical properties of large samples of objects (e.g., CRE age distribution of meteorites) or qualitative arguments (e.g., origin of large NEAs, size-dependent dispersion of the asteroid families). To conclusively prove the existence of the Yarkovsky effect, however, it would be useful to directly detect its orbital perturbation on asteroids in a manner consistent with what was done for the LAGEOS artificial satellite (e.g., *Rubincam*, 1987). *Vokrouhlický and Milani* (2000) and *Vokrouhlický et al.* (2000) have suggested that the Yarkovsky perturbations can be computed directly from radar observations of small NEAs like (1566) Icarus, (6489) Golevka, or 1998 KY26 over a period of years. The advantages of radar include precise astrometry (by a factor of 100–1000 better than the usual optical astrometry), information on asteroid physical parameters like shape/surface properties, and its rotation state, all useful for Yarkovsky modeling efforts. At the time of this writing, the necessary plans—including possible pre-apparition optical observations—are underway. If the modeling work of *Vokrouhlický et al.* (2000) is correct, radar observations during the next close encounters of the most promising candidate asteroids may produce a discernable Yarkovsky “footprint”.

The biggest challenge for future Yarkovsky modeling will be combining Yarkovsky accelerations with YORP, particularly since there is a complicated interaction between rotation, orbit precession rates, and spin axis precession rates. For many asteroids, particularly those km-sized and larger, the spin and orbital precession rates are comparable, such that we can expect complicated beat-like phenomena to affect obliquity over relatively short timescales (*Skoglov*, 1999). Moreover, coupling between the rates may allow the spin axis to be captured into a spin-orbit resonance. All of these factors produce complicated feedbacks which (i) can modify asteroid drift rates and rotation rate changes and (ii) are difficult to predict without extensive modeling. Since YORP is sensitive to the size, shape, material properties, and asteroid location, this effect will also vary from object to object. Thus, though we have hopefully demonstrated the usefulness of including Yarkovsky forces into the classical asteroid evolution model, there is still much work left to be done.

## REFERENCES

- Afonso G. B., Gomes R. S., and Florczak M. A. (1995) Asteroid fragments in Earth-crossing orbits. *Planet. Space Sci.*, 43, 787-795.
- Benz W., and Asphaug E. (1999) Catastrophic disruptions revisited. *Icarus*, 142, 5-20.
- Bendjoya. (2002) Asteroid families. In *Asteroids III* (W. Bottke *et al.*, eds.), this volume, Univ. of Arizona, Tucson.
- Binzel R. P., Farinella P., Zappalà V., and Cellino A. (1989) Asteroid rotation rates - Distributions and statistics. In *Asteroids II* (R. P. Binzel, T. Gehrels, and M. S. Matthews, eds.) pp. 416-441, Univ. of Arizona, Tucson.
- Binzel R. P., Harris A. W., Bus S. J., and Burbine T. H. (2001) Spectral properties of near-Earth objects: Palomar and IRTF results for 48 objects including spacecraft targets (9969) Braille and (10302) 1989 ML. *Icarus*, 151, 139-149.
- Bottke W. F., Nolan M. C., Greenberg R., and Kolvoord R. A. (1994) Velocity distributions among colliding asteroids. *Icarus*, 107, 255-268.
- Bottke W. F., Jedicke R., Morbidelli A., Petit J., and Gladman B. (2000a) Understanding the distribution of near-Earth asteroids. *Science*, 288, 2190-2194.
- Bottke W. F., Rubincam D. P., and Burns J. A. (2000b) Dynamical evolution of main belt meteoroids: Numerical simulations incorporating planetary perturbations and Yarkovsky thermal forces. *Icarus*, 145, 301-331.
- Bottke W. F., Morbidelli A., Jedicke R., Petit J.-M., Levison, H., Michel, P., and Metcalfe, T. S. (2001a) Debaised orbital and size distributions of Near-Earth objects. *Icarus*, in press.
- Bottke, W. F., Vokrouhlický, D. Brož, M., and Morbidelli, A. (2001b) Yarkovsky-assisted escape of kilometer-sized asteroids from the main belt. *Icarus*, in preparation.
- Brož M., Vokrouhlický D. and Farinella P. (2001) Interaction of the Yarkovsky-driven orbits of meteoroids and their precursors with the weak resonances in the main belt. *Icarus*, in preparation.
- Burns J. A., Lamy P. L., and Soter S. (1979) Radiation forces on small particles in the solar system. *Icarus*, 40, 1-48.
- Caffee M. W., Reedy R. C., Goswami J. N., Hohenberg C. M., and Marti K. (1988) Irradiation records in meteorites. In *Meteorites and the Early Solar System*, (J. F. Kerridge and M. S. Matthews, eds.) pp. 205-245. Univ. of Arizona Press, Tucson.
- Carruba V., Burns J. A., Bottke W.F., and Morbidelli A. (2000) Asteroid mobility due to encounters with Ceres, Vesta, Pallas: Monte Carlo codes versus direct numerical integrations. *AAS/Division of Planetary Sciences Meeting*, 32, 1406.

- Cellino A., Michel P., Tanga P., Zappalà V., Paolicchi P., and dell'Oro A. (1999) The velocity-size relationship for members of asteroid families and implications for the physics of catastrophic collisions. *Icarus*, 141, 79-95.
- Davis D. R., Weidenschilling S. J., Farinella P., Paolicchi P., and Binzel R. P. (1989) Asteroid collisional history - Effects on sizes and spins. In *Asteroids II* (R. P. Binzel, T. Gehrels, and M. S. Matthews, eds.) pp. 805-826, Univ. of Arizona, Tucson.
- Dermott, S. (2002) Asteroidal dust. In *Asteroids III* (W. Bottke *et al.*, eds.), this volume, Univ. of Arizona, Tucson.
- Dohnanyi J. S. (1978) Particle dynamics. *Cosmic Dust* (J.A.M. McDonnell, ed.) Chichester, Sussex, England and New York, Wiley-Interscience, pp. 527-605.
- Dones, L., Gladman, B. Melosh, H. J., Tonks, W. B., Levison, H. F., and Duncan, M. (1999) Dynamical lifetimes and final fates of small bodies: Orbit integrations vs Öpik calculations. *Icarus* 142, 509-524.
- Farinella P., Gonczi R., Froeschlé Cl., and Froeschlé Ch. (1993) The injection of asteroid fragments into resonances. *Icarus*, 101, 174-187.
- Farinella P., Froeschlé C., Froeschlé C., Gonczi R., Hahn G., Morbidelli A., and Valsecchi G. B. (1994) Asteroids falling onto the Sun. *Nature*, 371, 315-316.
- Farinella P., Vokrouhlický D., and Hartmann W. K. (1998a) Meteorite delivery via Yarkovsky orbital drift. *Icarus*, 132, 378-387.
- Farinella P., Davis D., and Marzari F. (1998b) Why we are not hydrocode believers (yet). *Fifth workshop on catastrophic disruption in the solar system*. Abstract.
- Farinella P., and Vokrouhlický D. (1999) Semimajor axis mobility of asteroidal fragments. *Science*, 283, 1507-1510.
- Gladman B. J., Migliorini F., Morbidelli A., Zappalà V., Michel P., Cellino A., Froeschlé C., Levison H. F., Bailey M., and Duncan M. (1997) Dynamical lifetimes of objects injected into asteroid belt resonances. *Science*, 277, 197-201.
- Grieve, R. A. F., and Shoemaker E. M. (1994) The record of past impacts on Earth. In *Hazards Due to Comets and Asteroids* (T. Gehrels, M. S. Matthews, eds.) pp. 417-462, Univ. of Arizona, Tucson.
- Hartmann W. K., Farinella P., Vokrouhlický D., Weidenschilling S. J., Morbidelli A., Marzari F., Davis D. R., and Ryan E. (1999) Reviewing the Yarkovsky effect: New light on the delivery of stone and iron meteorites from the asteroid belt. *Meteorit. and Planet. Sci.*, 34, 161-167.

- Knežević Z., Milani A., and Farinella P. (1997) The dangerous border of the 5:2 mean motion resonance. *Planet. Space Sci.*, 45, 1581-1585.
- Komarov M. M., and Sazonov V. V. (1994) The calculation of the forces and the torques caused by the solar light pressure acting on an arbitrary shaped asteroid. *Astr. Vestnik*, 28, 21-30.
- Katasev, L. A., and Kulikova, N. V. (1980) Physical and mathematical modeling of the formation and evolution of meteor streams II. *Astr. Vestnik*, 14, 225-229.
- Levison H. F., and Duncan M. J. (1994) The long-term dynamical behavior of short-period comets. *Icarus*, 108, 18-36.
- Marti K., and Graf T. (1992) Cosmic-ray exposure history of ordinary chondrites. *Ann. Rev. Earth Plan. Sci.*, 20, 221-243.
- Marzari F., Davis D., and Vanzani V. (1995) Collisional evolution of asteroid families. *Icarus*, 113, 168-187.
- Marzari F., Farinella P., and Davis D. R. (1999) Origin, aging, and death of asteroid families. *Icarus*, 142, 63-77.
- Michel P., Migliorini F., Morbidelli A., and Zappalà V. (2000) The population of Mars-Crossers: Classification and dynamical evolution. *Icarus*, 145, 332-347.
- Michel, P., Benz, W., Tanga, P., and Richardson, D. C. ( 2001) Collisions and gravitational re-accumulation: a recipe for forming asteroid families and satellites. *Science*, submitted.
- Migliorini F., Morbidelli A., Zappalà V., Gladman B. J., Bailey M. E., and Cellino A. (1997) Vesta fragments from  $\nu_6$  and 3:1 resonances: Implications for V-type NEAs and HED meteorites. *Meteorit. Planet. Sci.*, 32, 903-916.
- Migliorini F., Michel P., Morbidelli A., Nesvorný D., and Zappalà V. (1998) Origin of Earth-crossing asteroids: a quantitative simulation. *Science*, 281, 2022-2024.
- Milani A., and Farinella P. (1995) An asteroid on the brink. *Icarus*, 115, 209-212.
- Morbidelli A., and Gladman B. (1998) Orbital and temporal distributions of meteorites originating in the asteroid belt. *Meteorit. and Planet. Sci.*, 33, 999-1016.
- Morbidelli A., and Nesvorný D. (1999) Numerous weak resonances drive asteroids toward terrestrial planets orbits. *Icarus*, 139, 295-308.
- Neiman, V. B., Romanov, E. M., and Chernov, V. M. (1965) Ivan Osipovich Yarkovsky. *Earth and Universe (Russian magazine)*, No. 4, 63-64. (Translation into English by T. O. Laoghog available).

- Nesvorný, D., Morbidelli, A., Vokrouhlický, D., Bottke, W. F., and Brož, M. (2001) The Flora family: A case of the dynamically dispersed collisional swarm? *Icarus*, in press.
- O'Keefe J. A. (1976) Tektites and their origin. *Developments in Petrology*, No. 4 Amsterdam, Elsevier.
- Olsson-Steel D. (1986) The origin of the sporadic meteoroid component. *MNRAS*, 219, 47-73.
- Olsson-Steel D. (1987) The dispersal of the Geminid meteoroid stream by radiative effects. *MNRAS*, 226, 1-17.
- Öpik E. J. (1951) Collision probabilities with the planets and the distribution of interplanetary matter. *Proc. R. Irish Acad.*, 54A, 165-199.
- Öpik E. J. (1976) *Interplanetary encounters*. New York, NY, Elsevier.
- Paddack S. J. (1969) Rotational bursting of small celestial bodies: effects of radiation pressure. *J. Geophys. Res.*, 74, 4379-4381.
- Paddack S. J. (1973) Rotational bursting of small particles. Ph.D. thesis, Catholic University, Washington, D. C.
- Paddack S. J., Rhee J. W. (1975) Rotational bursting of interplanetary dust particles. *Geophys. Res. Lett.*, 2, 365-367.
- Peterson C. (1976) A source mechanism for meteorites controlled by the Yarkovsky effect. *Icarus*, 29, 91-111.
- Pisani E., dell'Oro A., and Paolicchi P. (1999) Puzzling asteroid families. *Icarus*, 142, 78-88.
- Pravec P., and Harris A. W. (2000) Fast and slow rotation of asteroids. *Icarus*, 148, 12-20.
- Pravec, P., AND CO-AUTHORS. (2002) Spin rates of asteroids. In *Asteroids III* (W. Bottke *et al.*, eds.), this volume, Univ. of Arizona, Tucson.
- Radzievskii V. V. (1952) About the influence of the anisotropically reemitted solar radiation on the orbits of asteroids and meteoroids. *Astron. Zh.*, 29, 162-170.
- Radzievskii V. V. (1954) A mechanism for the disintegration of asteroids and meteorites. *Dokl. Akad. Nauk SSSR*, 97, 49-52.
- Rubincam D. P. (2000) Radiative spin-up and spin-down of small asteroids. *Icarus*, 148, 2-11.
- Rubincam D. P. (1998) Yarkovsky thermal drag on small asteroids and Mars-Earth delivery. *J. Geophys. Res.*, 103, 1725-1732.
- Rubincam D. P. (1995) Asteroid orbit evolution due to thermal drag. *J. Geophys. Res.*, 100, 1585-1594.



- Rubincam D. P. (1990) Drag on the LAGEOS satellite. *J. Geophys. Res.*, *95*, 4881-4886.
- Rubincam D. P. (1988) Yarkovsky thermal drag on LAGEOS. *J. Geophys. Res.*, *93*, 13805-13810.
- Rubincam D. P. (1987) LAGEOS orbit decay due to infrared radiation from earth. *J. Geophys. Res.*, *92*, 1287-1294.
- Skoglov E. (1999) Spin vector evolution for inner solar system asteroids. *Planet. Space Sci.*, *47*, 11-22.
- Slabinski V. J. (1977) Solar radiation torques on meteoroids: complications for the Yarkovsky effect from spin axis precession. *BAAS*, *9*, 438.
- Slabinski V. J. (1996) A Numerical solution for LAGEOS thermal thrust: the rapid-spin case. *Celest. Mech. and Dyn. Astr.*, *66*, 131-179.
- Spitale J., and Greenberg R. (2001a) Numerical evaluation of the general Yarkovsky effect: Effects on semimajor axis. *Icarus*, *149*, 222-234.
- Spitale J., and Greenberg R. (2001b) Numerical evaluation of the general Yarkovsky effect: Effects on eccentricity, inclination, and longitude of periapse. *Icarus*, in press.
- Tanga P., Cellino A., Michel P., Zappalá V., Paolicchi P., and dell'Oro A. (1999) On the size distribution of asteroid families: The role of geometry. *Icarus*, *141*, 65-78.
- Vokrouhlický D. (1998a) Diurnal Yarkovsky effect as a source of mobility of meter-sized asteroidal fragments. I. Linear theory. *Astron. Astrophys.*, *335*, 1093-1100.
- Vokrouhlický D. (1998b) Diurnal Yarkovsky effect as a source of mobility of meter-sized asteroidal fragments. II. Non-sphericity effects. *Astron. Astrophys.*, *338*, 353-363.
- Vokrouhlický D. (1999) A complete linear model for the Yarkovsky thermal force on spherical asteroid fragments. *Astron. Astrophys.*, *344*, 362-366.
- Vokrouhlický D. (2001) Yarkovsky effect: Many-fingered phenomenon in the solar system dynamics. In *The Restless Universe: Applications of Gravitational N-Body Dynamics to Planetary, Stellar and Galactic Systems*, (B.A. Steves and A.E. Roy, eds.), Institute of Physics, London, in press.
- Vokrouhlický D., and Farinella P. (1998) The Yarkovsky seasonal effect on asteroidal fragments: A nonlinearized theory for the plane-parallel case. *Astron. J.*, *116*, 2032-2041.
- Vokrouhlický D., and Farinella P. (1999) The Yarkovsky seasonal Effect on asteroidal fragments: A nonlinearized theory for spherical bodies. *Astron. J.*, *118*, 3049-3060.
- Vokrouhlický D., and Brož, M. (1999) An improved model of the seasonal Yarkovsky force for regolith-covered asteroid fragments. *Astron. Astrophys.*, *350*, 1079-1084.

- Vokrouhlický D., and Farinella P. (2000) Efficient delivery of meteorites to the Earth from a wide range of asteroid parent bodies. *Nature*, 407, 606-608.
- Vokrouhlický D., and Milani A. (2000) Direct solar radiation pressure on the orbits of small near-Earth asteroids: Observable effects? *Astron. Astrophys.*, 362, 746-755.
- Vokrouhlický D., and Bottke W. F. (2001) The Yarkovsky thermal force on small asteroids and their fragments. Choosing the right albedo. *Astron. Astrophys.*, 371, 350-353.
- Vokrouhlický D. and Čapek D. (2001) YORP-induced long-term evolution of the spin state of small asteroids and meteoroids. I. Rubincam's approximation. *Icarus*, submitted.
- Vokrouhlický D., Milani A., and Chesley S. R. (2000) Yarkovsky effect on small near-Earth asteroids: Mathematical formulation and examples. *Icarus*, 148, 118-138.
- Vokrouhlický D., Brož M., Farinella P., and Knežević Z. (2001) Yarkovsky-driven leakage of Koronis family members. *Icarus*, 150, 78-93.
- Welten K. C., Lindner L., van der Borg K., Loeken T., Scherer P., and Schultz L. (1997) Cosmic-ray exposure ages of diogenites and the recent collisional history of the HED parent body/bodies. *Meteorit. and Planet. Sci.*, 32, 891-902.
- Wetherill G. W. (1974) Solar system sources of meteorites and large meteoroids. *Ann. Rev. Earth Plan. Sci.*, 2, 303-331.
- Wetherill G. W. (1979) Steady state populations of Apollo-Amor objects. *Icarus*, 37, 96-112.
- Wetherill G. W. (1985) Asteroidal source of ordinary chondrites (Meteoritical Society Presidential Address 1984). *Meteoritics*, 20, 1-22.
- Whipple F. L. (1950) A comet model. I. The acceleration of Comet Encke. *Astrophys. J.*, 111, 375-394.
- Wisdom J. (1983) Chaotic behavior and the origin of the 3/1 Kirkwood gap. *Icarus*, 56, 51-74.
- Wisdom J., Holman M. (1991) Symplectic maps for the n-body problem. *Astron. J.*, 102, 1528-1538.
- Zappalà V., and Cellino A. (2001) A search for the collisional parent bodies of large NEAs. *Icarus*, in press.
- Zappalà V., Bendjoya P., Cellino A., Farinella P., and Froeschlé C. (1995) Asteroid families: Search of a 12,487-asteroid sample using two different clustering techniques. *Icarus*, 116, 291-314.
- Zappalà V., Cellino A., dell'Oro A., Migliorini F., and Paolicchi P. (1996) Reconstructing the original ejection velocity fields of asteroid families. *Icarus*, 124, 156-180.

Zappalà V., Cellino A., Gladman B. J., Manley S., and Migliorini F. (1998) NOTE: Asteroid showers on Earth after family breakup events. *Icarus*, 134, 176-179.

Zappalà V., Bendjoya P., Cellino A., Di Martino M., Doressoundiram A., Manara A., and Migliorini F. (2000) Fugitives from the Eos family: First spectroscopic confirmation. *Icarus*, 145, 4-11.

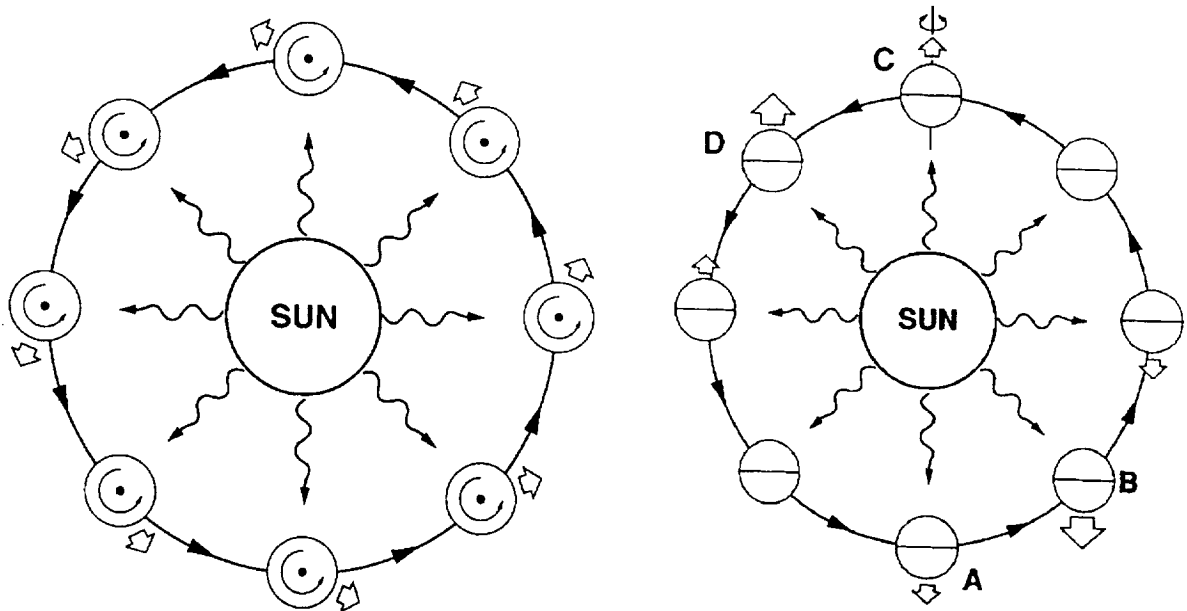


Fig. 1.— (a) The diurnal Yarkovsky effect, with the asteroid's spin axis perpendicular to the orbital plane. A fraction of the solar insolation is absorbed only to later be radiated away, yielding a net thermal force in the direction of the wide arrows. Since thermal reradiation in this example is concentrated at about 2 PM on the spinning asteroid, the radiation recoil force is always oriented at about 2 AM. Thus, the along-track component causes the object to spiral outward. Retrograde rotation would cause the orbit to spiral inward. (b) The seasonal Yarkovsky effect, with the asteroid's spin axis in the orbital plane. Seasonal heating and cooling of the "northern" and "southern" hemispheres give rise to a thermal force which lies along the spin axis. The strength of the reradiation force varies along the orbit as a result of thermal inertia; even though the maximum sunlight on each hemisphere occurs as A and C, the maximum resultant radiative forces are applied to the body at B and D. The net effect over one revolution always causes the object to spiral inward.

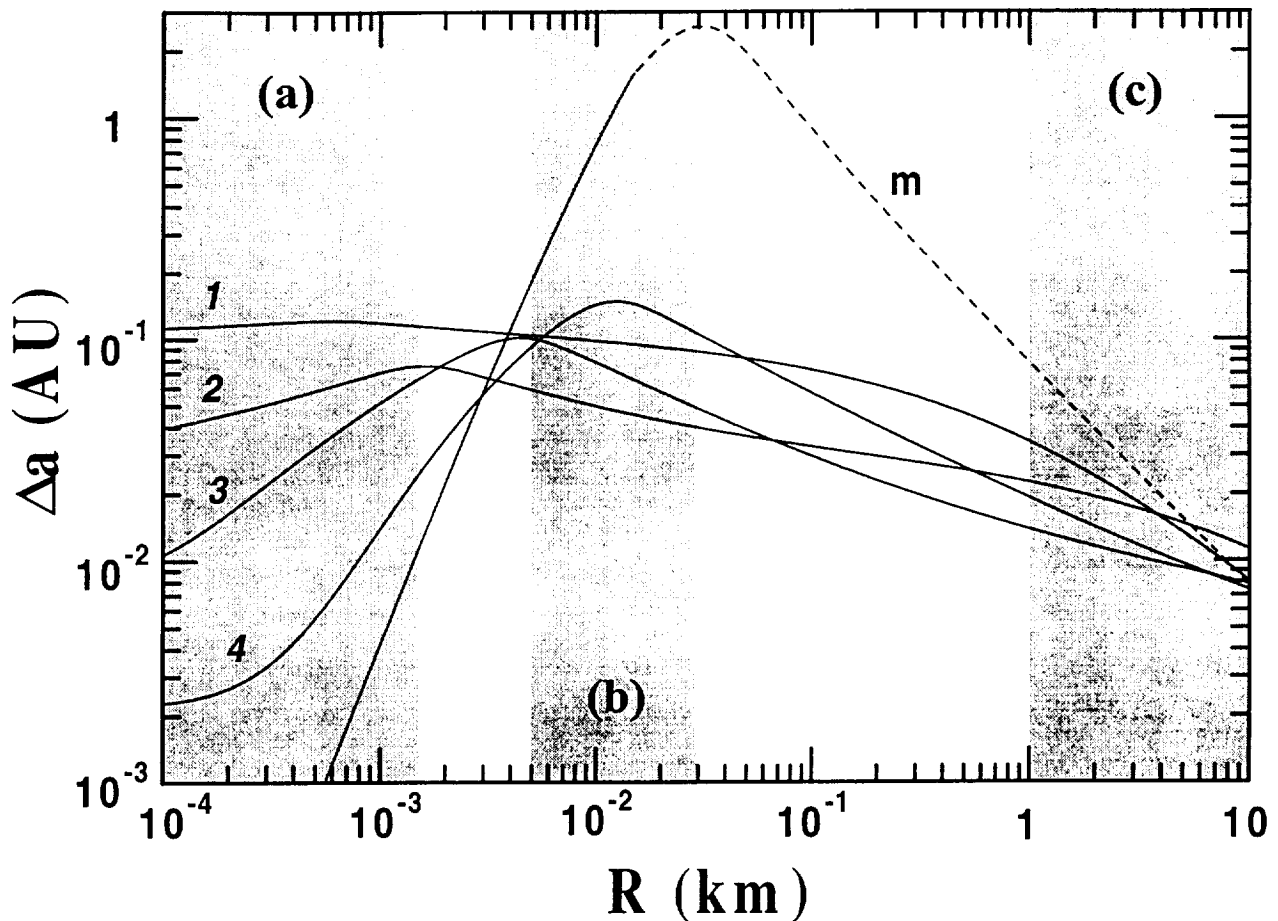


Fig. 2.— Mean change of the semimajor axis  $\Delta a$  (in AU) of inner main belt asteroids over their collisional lifetimes (see text) vs. their radius  $R$  (in km). Both components (diurnal and seasonal) of the Yarkovsky effect are included. Five different values of the surface conductivity  $K$  are considered: (1)  $K = 0.002$  W/m/K; (2)  $K = 0.02$  W/m/K; (3)  $K = 0.2$  W/m/K; (4)  $K = 2$  W/m/K; and  $K = 40$  W/m/K (curve  $m$ , for metal-rich bodies). The low- $K$  cases are dominated by the diurnal effect, while for high- $K$  cases the seasonal effect is more important. The dashed strips correspond to three astronomically important classes of bodies: (a) pre-atmospheric meteorite parent bodies ( $R = 0.1$ – $1.5$  m); (b) Tunguska-like small NEAs ( $R = 5$ – $30$  m); and (c) the largest existing NEAs or the smallest observed family members ( $R = 1$ – $10$  km). Note that  $\Delta a$  depends sensitively on the selected value of  $K$  in the (a) and (b) size ranges, but much less so in range (c).

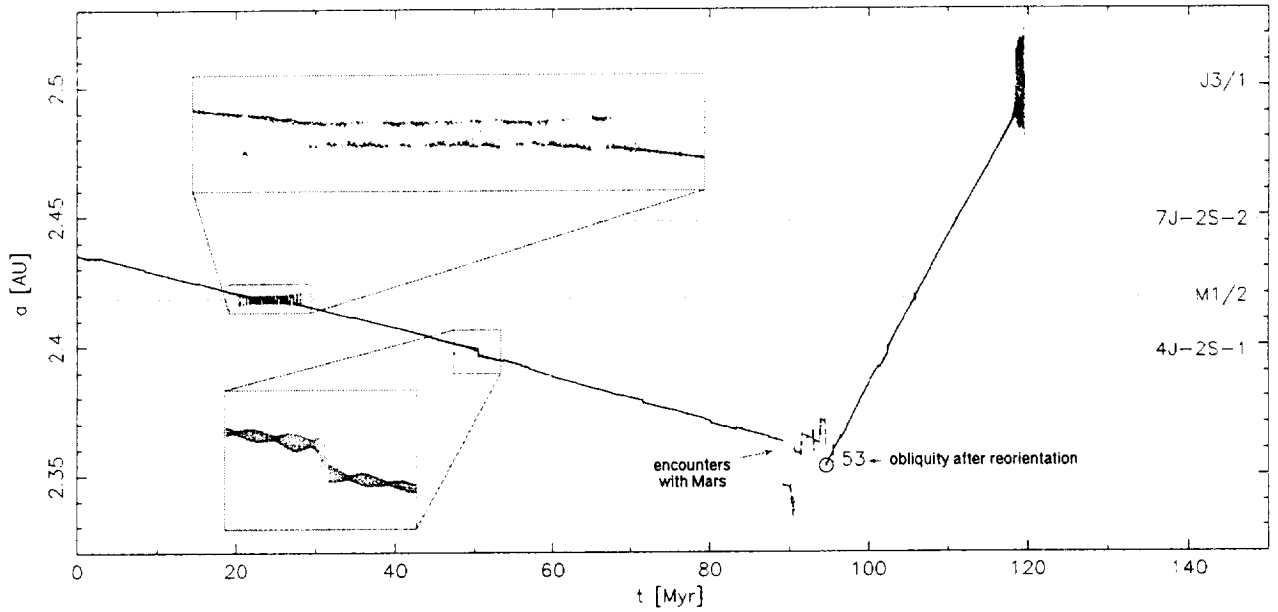


Fig. 3.— Mean semimajor axis (in AU) vs. time for a 20m asteroid ejected from asteroid (6) Hebe. A low-conductivity surface is assumed. Periods of interaction with weak resonances are magnified in the two boxes: (i) temporary capture in the 1:2 mean-motion resonance with Mars, lasting for about 10 Myr, and (ii) rapid jump over the Jupiter-Saturn-asteroid mean-motion resonance (4,-2,-1). At  $\approx 90$  Myr the orbit was weakly scattered on Mars (due to close encounters), but the spin axis was reoriented by a collision at the same time. Within next  $\approx 30$  Myr, the asteroid crossed the inner part of the asteroid belt and was ejected via the 3:1 resonance.

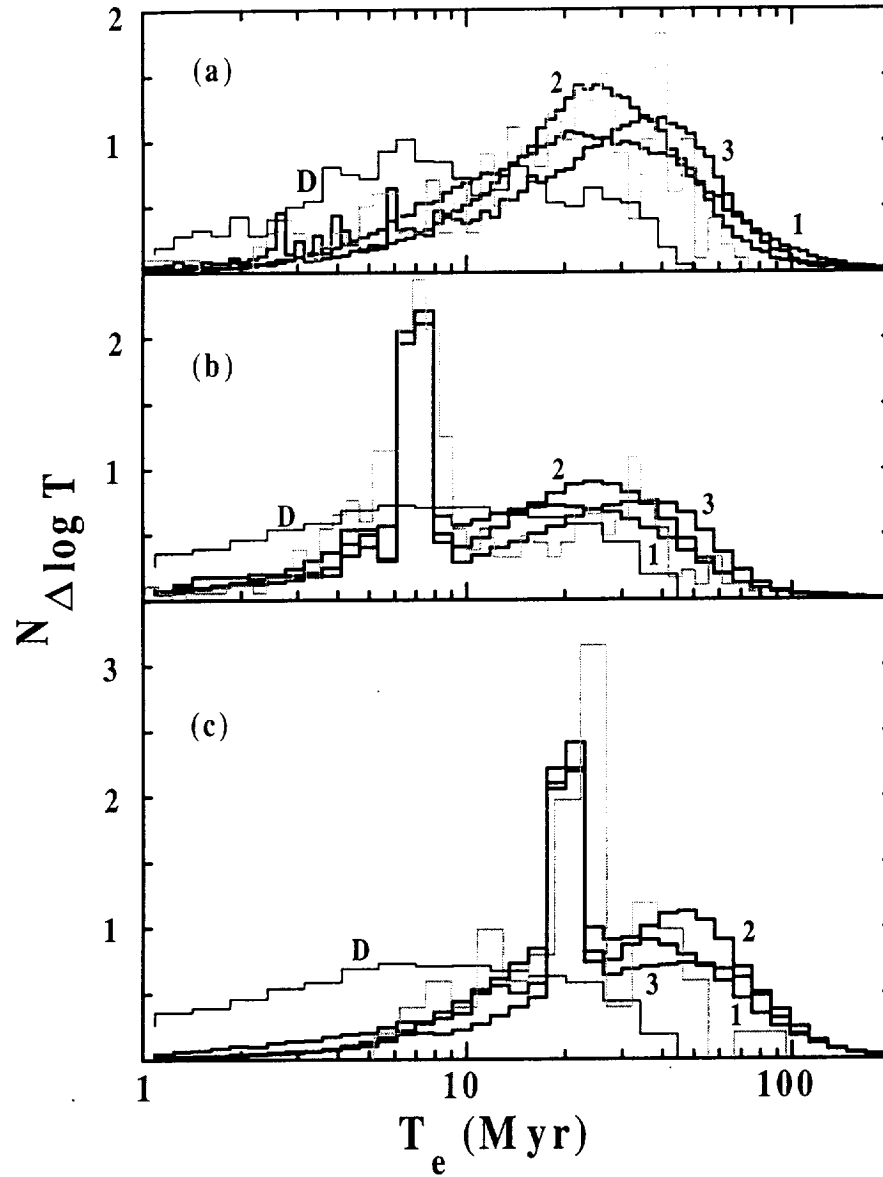


Fig. 4.— Comparison of the modeled and observed CRE-age distributions for three different meteorite types (data – grey histograms). We show results of the direct-injection scenario with no Yarkovsky mobility (D histogram) and the model including Yarkovsky mobility of the meteoroids and their precursors (bold full-line histograms). Histograms 1, 2 and 3 refer to thermal conductivity values of 0.0015, 0.1 and 1 W/m/K, respectively. Part (a) assumes ejecta from asteroid Flora whose computed CRE ages are compared with the observed distribution for 240 L-chondrites. Part (b) assumes ejecta from asteroid (6) Hebe and the comparison with 444 CRE ages of H-chondrites. Part (c) assumes ejecta from asteroid (4) Vesta, compared to the CRE age data for 64 HED (howardite-eucrite-diogenite) meteorites. In all cases, the intermediate  $K$  value appears to provide the best match to the data. Note that the direct injection scenario would always predict many more short CRE ages than are observed, and a shortage of ages between 20 and 50 Myr, which is not observed.

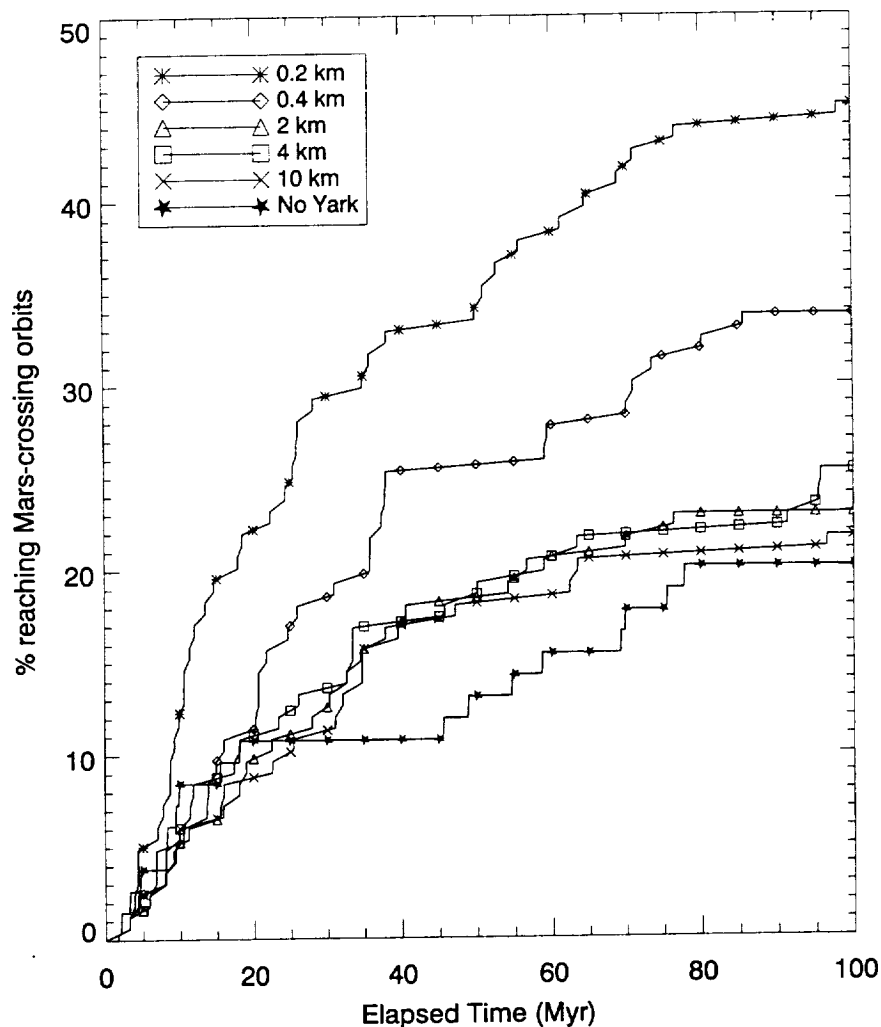


Fig. 5.— Evolution of nearly-Mars-crossing bodies under the influence of Yarkovsky thermal forces. The plot shows the fraction test asteroids, started with perihelion  $q \gtrsim 1.8$  AU, reaching Mars-crossing orbits after 100 Myr of integration. The initial conditions of the test asteroids nearly duplicated the initial conditions of *Morbidelli and Nesvorný* (1999). The bottom-curve shows the *Morbidelli and Nesvorný* (1999) results. Results indicate that roughly the same fraction of  $D > 2$  km bodies reach Mars-crossing orbits after 100 Myr, with or without Yarkovsky. Asteroids with  $D < 2$  km, however, are much more efficient at escaping the main belt.



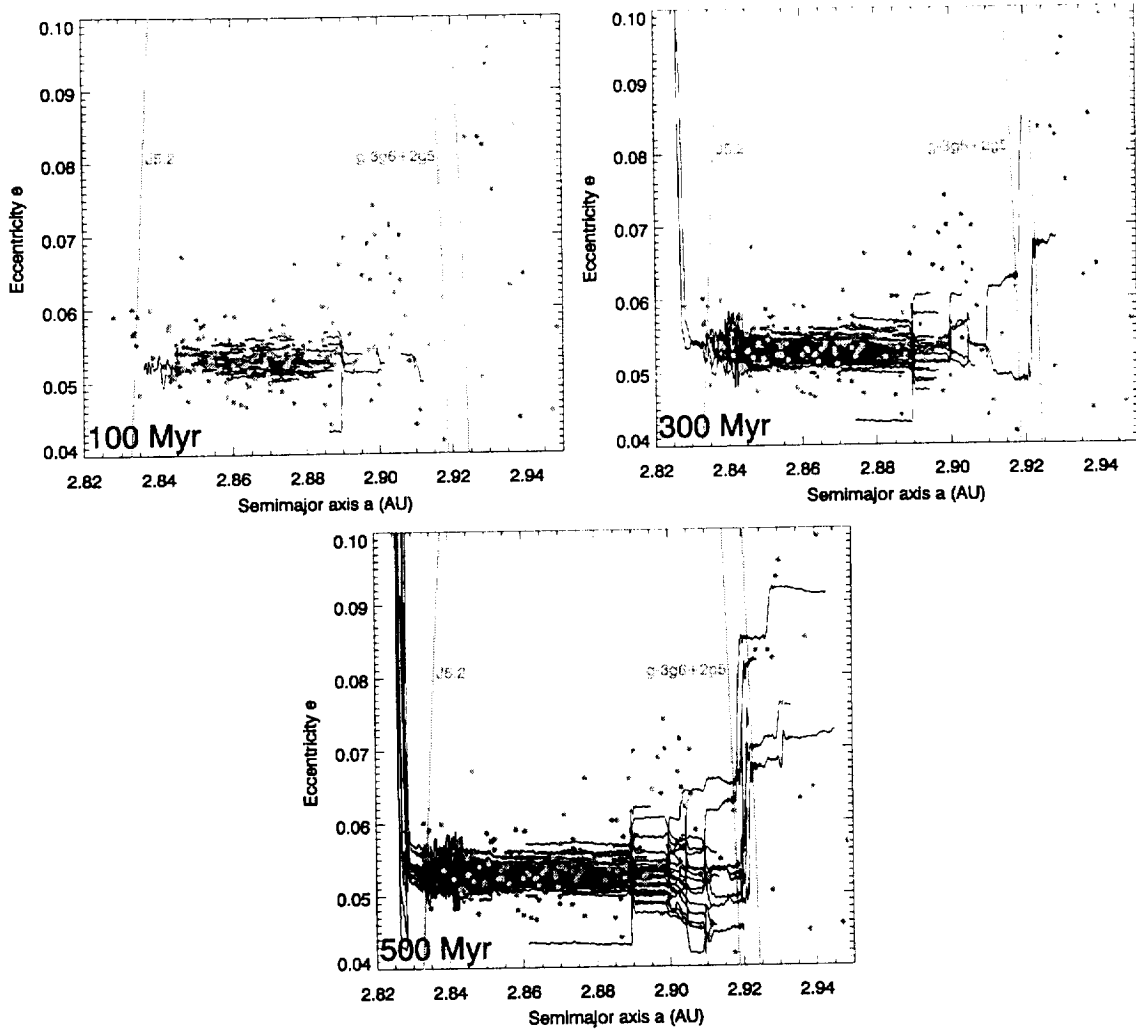


Fig. 6.— Evolution of 210 fake Koronis family members via the Yarkovsky effect. The test asteroids (dark lines) were started within  $\sim 60 \text{ m s}^{-1}$  of (158) Koronis and were integrated for 500 Myr. The orbital tracks were averaged over a running 10 Myr window, such that they represent evolution in “proper”  $a$  and  $e$ . The grey points represent the proper  $a$  and  $e$  of the Koronis family members identified by Zappalà *et al.* (1995). The fake Koronis family members were given random size axis orientations, diameters between  $2 < D < 20 \text{ km}$ , and thermal properties consistent with regolith-covered surfaces. The integration tracks show these bodies interact with by several tiny secular resonances between 2.9–2.93 AU, with the  $g - 3g_6 + 2g_5$  resonance being most prominent. These jumps allow the fake family members to reach the  $(a, e)$  positions of many real family members. In addition, the largest (and fastest) jumps are not associated with known family members, providing some support for an drifting family scenario. Fake asteroids also escape the main belt via the 5:2 mean-motion resonance with Jupiter (outer boundary near  $\sim 2.83 \text{ AU}$ ). Mismatches between observations and integration data are discussed in the text.

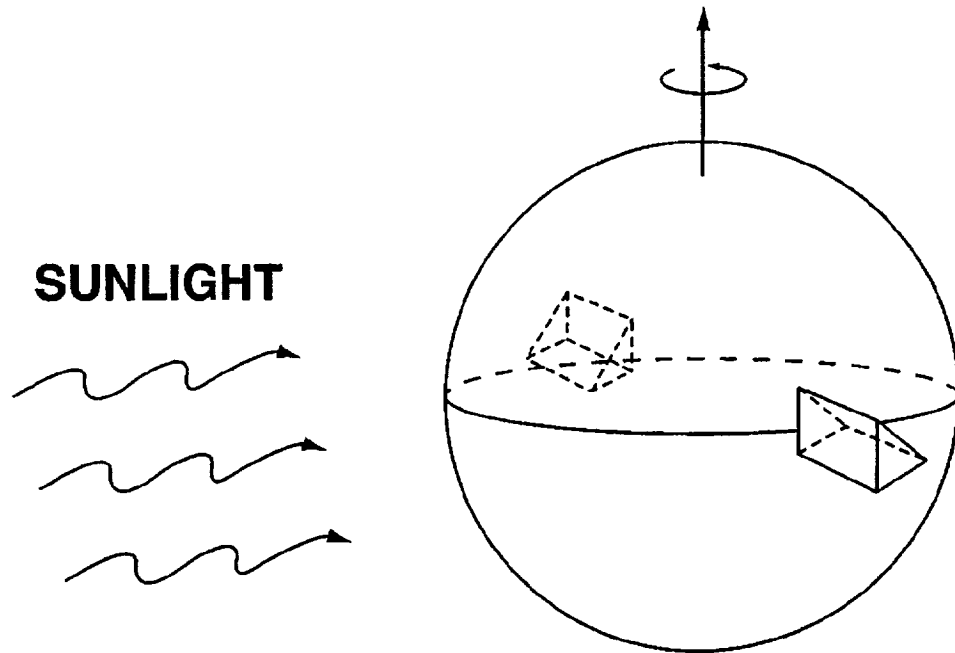


Fig. 7.— Spin up of an asymmetrical asteroid. The asteroid is modeled as a sphere with two wedges attached to its equator. The asteroid is considered a blackbody, so it absorbs all sunlight falling upon it and then reemits the energy in the infrared as thermal radiation. Since the kicks produced by photons leaving the wedges are in different directions, a net torque is produced which causes the asteroid to spin up.